Design and Analysis of a Butler Matrix at 60 GHz Compatible with Metallic-Nanowire-Filled Membrane Fabrication Platform

Elígia Simionato, Bruno M. Verona, Marcela Pires, Ivan Aldaya, José A. Oliveira, Ariana L. C. Serrano, Gustavo P. Rehder and Rafael A. Penchel

***Abstract*— This work describes the design and analysis of a 4×4 Butler matrix for applications in the 60 GHz unlicensed frequency band. Each of the constitutive blocks that make up the network – hybrid coupler, crossover, and phase shifter – were designed to be compatible with metallic-nanowire-filled membrane manufacturing process and optimized separately. Simulations were conducted using Ansys HFSS and improvements to the devices' behaviours were achieved through parametric analysis. A complete design was obtained by connecting all primary devices and each output port was connected to a series patch antenna array. The complete Butler matrix analysis revealed a device that produces the expected phase distribution and radiation at the desired angles.**

***Keywords*— Butler matrix, nanowire-filled-membrane, millimetre wave**

I. Introduction

The ever-growing demand for higher transmission rates by mobile systems and other wireless services such as fixed, broadcasting and satellite communications has made the crowded sub-6 GHz frequencies unattractive to develop innovative technology that highly depends on spectrum availability. In this sense, the 60 GHz band is particularly interesting because of the wide unlicensed spectrum ($\sim$7 GHz). However, the 57 – 64 GHz band corresponds to many oxygen absorption peaks [1], resulting in a high path loss and limited the transmission distance [2], [3]. Such high attenuation makes 60 GHz systems impractical for long range communication, yet allurring for transmission over typical indoor distances ($\sim$10 m). In fact, wireless local/personal area network (WLAN/WPAN) benefit from the attenuation, which provides extra spatial isolation (lower probability of interference) and higher implicit security [3].

Added to the attenuation caused by atmospheric gaseous, dust and rain, the path loss grows with the square of the carrier frequency with isotropic transmit and receive antennas [4]. In principle, the use of more directive antennas can compensate for the higher free space loss [5]. Hence, beamforming – adaptive electronically steerable beams – is one of the key techniques that will allow for mobility and improve the channel propagation characteristics at mm-Wave frequencies [3], [6].

A well-known beamforming network solution is the Butler matrix, which can provide, simultaneously, excellent matching, isolation and equal power division. Compared with other beamforming networks, the Butler matrix has some attractive features, such as a large bandwidth, a structural simplicity and a very low current consumption [7]. Butler matrices are composed of 90^o hybrid directional couplers, crossovers and fixed phase shifters. These primary components are interlaced in a way such that a signal introduced at one input produces a constant phase difference between all outputs, resulting in radiation at a certain angle in space [8], [9].

Reference [10] presents a generally known Butler matrix structure, with crossovers consisting of a combination of two couplers, which leads to an expansive device. A more compact design is reported in [11], where slow-wave microstrip lines are employed to reduce the size. A different crossover structure is used in [12] seeking a more compact device without miniaturization based on slow-wave technology.

The present work aims to design and analyse a 4×4 Butler matrix that can be implemented in metallic-nanowire-filled membrane (MnM) for applications in the 60 GHz band. MnM is a versatile high-frequency, low-cost interposer technology that shows great potential for the development of mm-Wave applications [13], [14]. The Butler matrix will be studied with four-element series patch antenna arrays connected to the output ports, as illustrated in Fig. 1. Section II outlines the general fabrication process using MnM technology. Section III describes the design process of the patch antenna array and each primary device that composes the Butler matrix, while Section IV presents the complete network analysis.

II. MnM technology

The MnM technology used in this work is based on a 50 μm-thick nanoporous Alumina substrate ($\epsilon_r = 6.7$, $\tan\delta = 0.015$). The first step of the MnM fabrication process of RF circuits and devices is a cleaning stage, which is followed by deposition of a thin copper film on the backside of the substrate. The front side of the substrate receives a silicon dioxide (SiO_2) mask, allowing selective growth of nanowires. Where the substrate is exposed through the SiO_2, nanowires

Elígia Simionato, FESJ/UNESP, São João da Boa Vista - SP, e-mail: e.simionato@unesp.br; Bruno M. Verona, USP, São Paulo - SP, e-mail: brunoverona@ipt.br; Marcela Pires, FESJ/UNESP, São João da Boa Vista - SP, e-mail: marcela.p.souza@unesp.br; Ivan Aldaya, FESJ/UNESP, São João da Boa Vista - SP, e-mail: ivan.aldaya@unesp.br; Ariana L. C. Serrano, USP, São Paulo - SP, e-mail: aserrano@usp.br; Gustavo P. Rehder, USP, São Paulo - SP, e-mail: gprehder@usp.br; Rafael A. Penchel, FESJ/UNESP, São João da Boa Vista - SP, e-mail: rafael.penchel@unesp.br. This work was supported by the following Brazilian research agencies: FAPESP, grant #2022/03519-6 and CNPq, grant #409146/2021-8

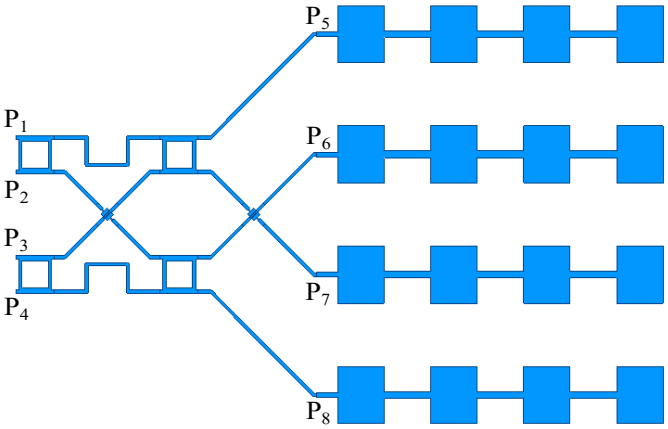

Fig. 1: Complete Butler matrix with series patch antenna arrays

are grown by electrodeposition, connecting both surfaces of the substrate in a simple fabrication process [13].

Previous works on millimetre wave devices using MnM technology [13], [14], [15] presented good agreement between measured and simulated results.

III. Butler Matrix Design

In this work, we adopted the Butler matrix design process described in [8], with each primary device – hybrid coupler, crossover, and phase shifter – and the four element fed-series patch array designed and optimazed separately, as described in the following sections.

For the 4 × 4 matrix shown in Fig. 1, two columns comprised by two hybrid couplers are necessary. Between the two columns, there is a crossover and two 45º phase shifters. Between the last column of hybrid couplers and the antenna arrays, there is one more crossover and two lines in-phase with the crossover (0º phase shifters). This configuration produces at the outputs, for each excited input, the phase values described in Table I.

TABLE I: Phase distribution at output ports for each input port

		Input ports			
		1	2	3	4
Out ports	5	-45º	-135º	-90º	-180º
	6	-90º	0º	-225º	-135º
	7	-135º	-225º	-0º	-90º
	8	-180º	-90º	-135º	-45º

All devices were simulated in Ansys HFSS with finite element method, and to improve the devices' behaviour, we employed parametric analysis.

A. Hybrid Couplers

The initial design for the 90º hybrid coupler (Fig. 2) was obtained following standard formulations [16], and the widths and lengths of the microstrip lines were adjusted to obtain the results shown in Fig. 3.

The hybrid coupler was analysed based on commonly used quantities: coupling, directivity, isolation, and insertion loss, defined in (1), (2), (3) and (4) [16], respectively. The reflection coefficient at each port and the phase difference between ports 2 and 3 (see Fig. 2) were also used to characterize the designed 90º hybrid coupler.

$$\text{Coupling} = C = -20\log|S_{13}| \text{ [dB]} \tag{1}$$

$$\text{Directivity} = D = 20\log\frac{|S_{13}|}{|S_{14}|} \text{ [dB]} \tag{2}$$

$$\text{Isolation} = I = -20\log|S_{14}| \text{ [dB]} \tag{3}$$

$$\text{Insertion loss} = L = -20\log|S_{12}| \text{ [dB]} \tag{4}$$

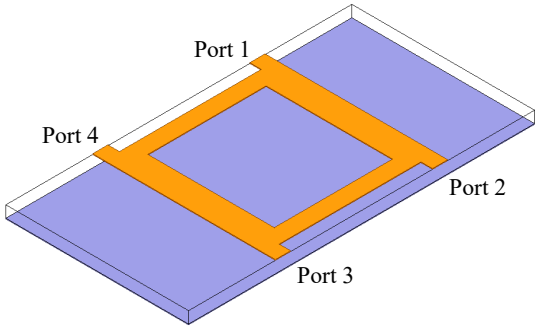

Fig. 2: Three-dimensional 90º hybrid coupler model

B. Crossovers and Phase Shifters

In this project we used the compact ultra-wideband crossover (Fig, 4) developed in [11], as it presents excellent performance for the intended application and is also based on MnM technology. We analysed its behaviour for the 60 GHz band and the results are displayed in Fig. 5. The most relevant feature of this crossover design is the negligible phase imbalance, shown in Fig. 5c, were 'line over' refers to the blue-coloured microstrip line in Fig. 4 and 'line under' is the orange-coloured line.

The phase shifters were implemented and analysed with the crossovers, as illustrated in Fig. 6, since the phase shift is determined in relation to the phase observed in the crossover lines. At 60 GHz, the phase difference between the 45º shifter and the crossover is 45.7º (Fig. 7a), and there is a 1º phase unbalance between the 0º shifter and the crossover (Fig. 7b).

C. Series Patch Antenna Arrays

To improve the gain of the beams generated by the Butler matrix, an array of equally spaced patch antennas (Fig. 8), distanced $\lambda_g/2$ from each other, was employed. Additionally, the design presents a $\lambda_g/4$ transformer (QWT) at the input to match the array's input impedance to a standard 50 Ω line.

Reflection coefficient and radiation pattern for the array are shown in Fig. 9.

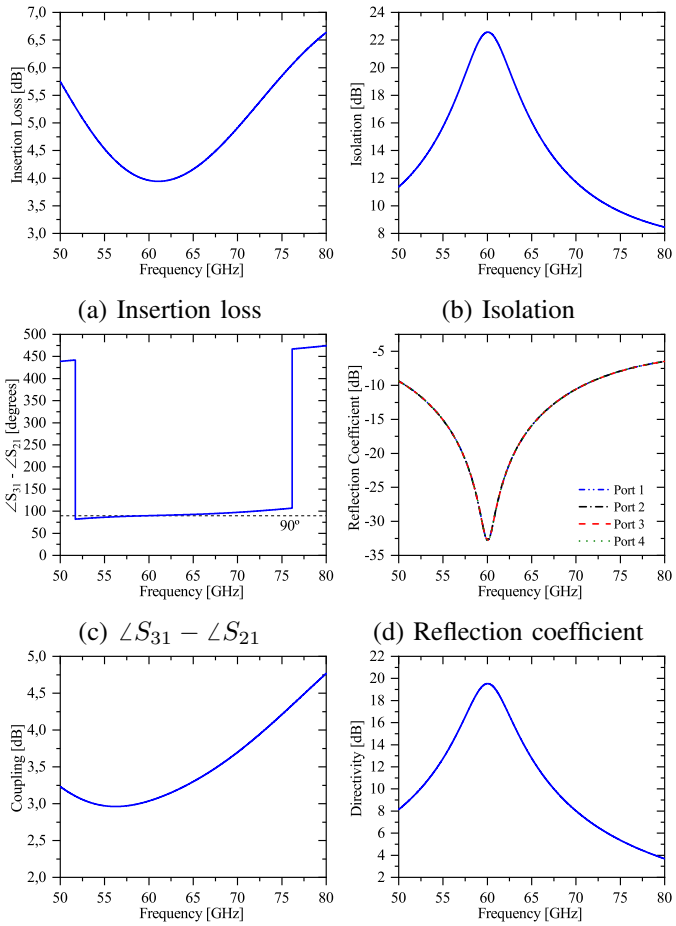

(a) Insertion loss (b) Isolation

(c) $\angle S_{31} - \angle S_{21}$ (d) Reflection coefficient

(e) Coupling (f) Directivity

Fig. 3: Hybrid coupler parameters

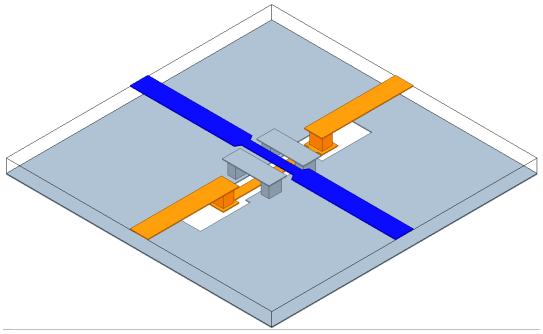

Fig. 4: Three-dimensional crossover model

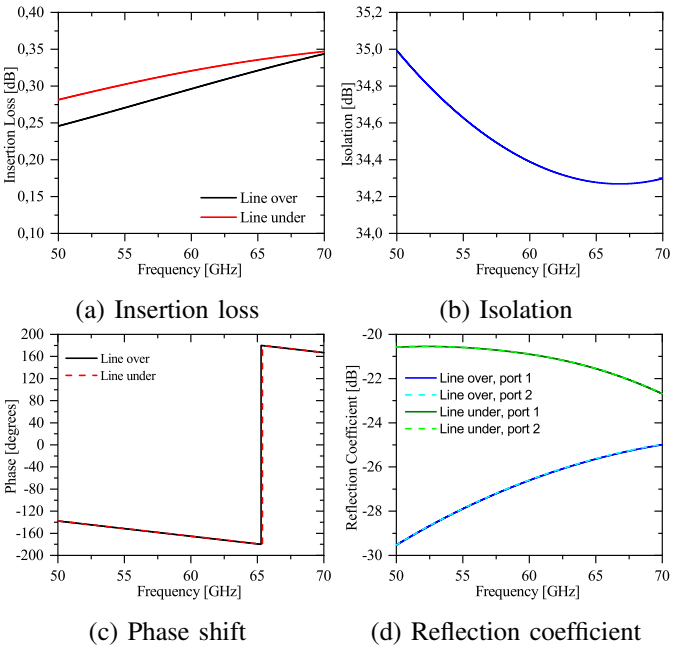

(a) Insertion loss (b) Isolation

(c) Phase shift (d) Reflection coefficient

Fig. 5: Crossover parameters

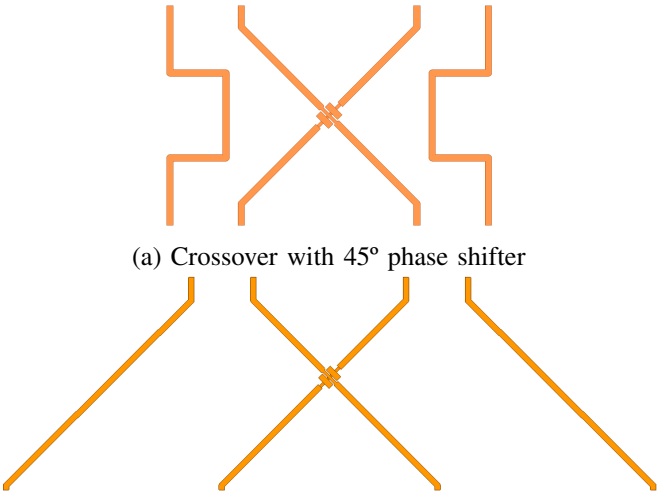

(a) Crossover with 45° phase shifter

(b) Crossover with 0° phase shifter

Fig. 6

IV. Complete Butler Matrix Analysis

The devices described in the preceding section, improved to produce the desirable results, were joined to form the complete Butler matrix, as seen in Fig. 1. The analysis of the network as a whole produced the results shown in Fig. 10.

The angles formed by the device's main beam, in relation to the broadside direction, are shown in Fig. 10b and highlighted in Table II. To validate this result, the ideal radiation pattern was obtained from a simulation considering only the four patch antenna array and introducing at the input of each array a signal with phase specified by Table I. This simulation disclosed a radiation pattern very similar to the one shown in Fig. 10b, and the ideal beam directions presented in Table II indicate a good convergence of the results. Additionally, Table II compares ideal and acquired beam direction with the results presented in [12], showing the systematic design process followed in this project yielded better results.

V. Conclusions

A complete Butler matrix design based on MnM technology was proposed for application in the 60 GHz band. The final design was obtained by analysing and improving the 90° hybrid couplers, crossovers, phase shifters and patch antenna arrays that compose the Butler matrix. The beam angle distribution acquired with the presented design almost exactly matches the ideal distribution, validating the design.

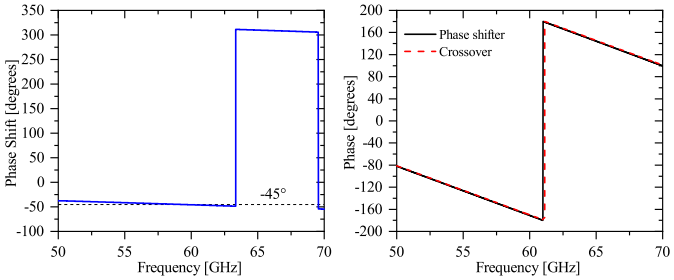

(a) 45º phase shifter (b) 0º phase shifter

Fig. 7: Phase shift

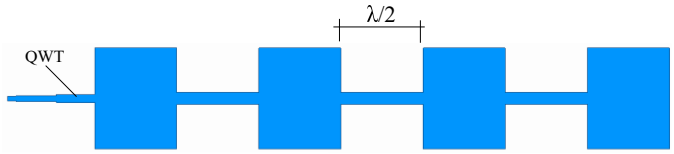

Fig. 8: Four-element series patch antenna array

REFERENCES

[1] M. Marcus and B. Pattan, "Millimeter wave propagation: spectrum management implications," *IEEE Microwave Magazine*, vol. 6, no. 2, pp. 54–62, Jun. 2005.

[2] J. Wells, "Faster than fiber: The future of multi-G/s wireless," *IEEE Microwave Magazine*, vol. 10, no. 3, pp. 104–112, May 2009.

[3] C. Doan, S. Emami, D. Sobel, A. Niknejad, and R. Brodersen, "Design considerations for 60 GHz CMOS radios," *IEEE Communications Magazine*, vol. 42, no. 12, pp. 132–140, Dec. 2004.

[4] L. Wei, R. Q. Hu, Y. Qian, and G. Wu, "Key elements to enable millimeter wave communications for 5G wireless systems," *IEEE Wireless Communications*, vol. 21, no. 6, pp. 136–143, Dec. 2014.

[5] P. Smulders, "Exploiting the 60 GHz band for local wireless multimedia access: prospects and future directions," *IEEE Communications Magazine*, vol. 40, no. 1, pp. 140–147, Jan. 2002.

[6] Z. Pi and F. Khan, "An introduction to millimeter-wave mobile broadband systems," *IEEE Communications Magazine*, vol. 49, no. 6, pp. 101–107, Jun. 2011.

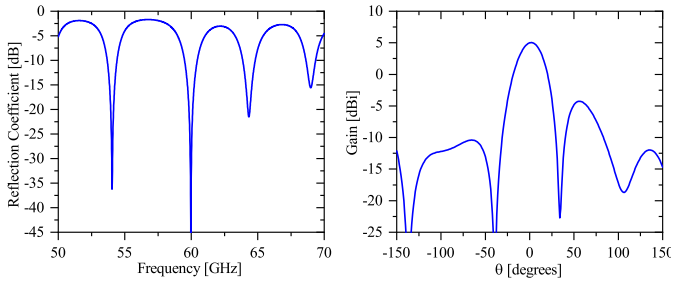

(a) Reflection coefficient (b) Radiation pattern ($\phi = 90º$)

Fig. 9: Four-element series patch antenna array parameters

TABLE II: Comparison of beam directions for each excited input port.

Input port	Ideal direction	Acquired direction	Direction presented in [12]
1	-13º	-13º	-14º
2	42º	41º	39º
3	-42º	-42º	-39º
4	13º	13º	13º

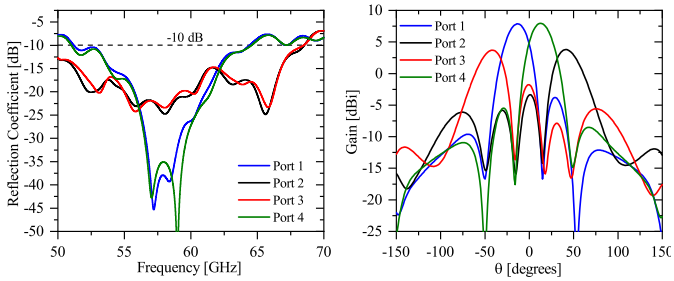

(a) Reflection coefficients (b) Radiation pattern

Fig. 10: Complete Butler matrix parameters

[7] G. Acri, "Sensitivity to technology and adjustability of substrate integrated waveguides Butler matrices, in PCB substrates at 28 GHz and in benzocyclobutene above-IC interposers at millimetre waves," Ph.D. dissertation, Jul. 2020.

[8] H. Moody, "The systematic design of the Butler matrix," *IEEE Transactions on Antennas and Propagation*, vol. 12, no. 6, pp. 786–788, Nov. 1964.

[9] W. P. Delaney, "An RF Multiple Beam-Forming Technique," *IRE Transactions on Military Electronics*, vol. MIL-6, no. 2, pp. 179–186, Apr. 1962.

[10] H. Nachouane, A. Najid, A. Tribak, and F. Riouch, "Broadband 4×4 Butler matrix using wideband 90° hybrid couplers and crossovers for beamforming networks," Apr. 2014, pp. 1444–1448.

[11] D. Wang, B. M. Verona, A. L. C. Serrano, P. Ferrari, R. Jakoby, H. Maune, and G. P. Rehder, "Compact DC to 110 GHz Crossover Based on Metallic-Nanowire-Filled Membrane," *IEEE Microwave and Wireless Components Letters*, vol. 32, no. 1, pp. 45–48, Jan. 2022.

[12] B. M. Verona, "Matriz de Butler em interposer MnM para aplicações em ondas milimétricas." text, Universidade de São Paulo, Sep. 2021. [Online]. Available: https://www.teses.usp.br/teses/disponiveis/3/3140/tde-31012022-123610/

[13] M. V. Pelegrini, J. M. Pinheiro, L. G. Gomes, G. P. Rehder, A. L. C. Serrano, F. Podevin, and P. Ferrari, "Interposer based on metallic-nanowire-membrane (MnM) for mm-wave applications," in *2016 11th European Microwave Integrated Circuits Conference (EuMIC)*, Oct. 2016, pp. 532–535.

[14] J. E. G. Lé, M. Ouvrier-Buffet, L. G. Gomes, R. A. Penchel, A. L. C. Serrano, and K. G. P. Rehder, "Integrated Antennas on MnM Interposer for the 60 GHz Band," *Journal of Microwaves, Optoelectronics and Electromagnetic Applications*, vol. 21, pp. 184–193, Mar. 2022. [Online]. Available: http://www.scielo.br/j/jmoea/a/Zm95w4WLFKVYp3cmZGjPJQJ/

[15] L. A. G. Gomes, "Projeto de antenas e caracterização do substrato de nanofios (MnM) para aplicações em ondas milimétricas." text, Universidade de São Paulo, Dec. 2017. [Online]. Available: http://www.teses.usp.br/teses/disponiveis/3/3140/tde-06042018-092811/

[16] D. Pozar, *Microwave Engineering, 4th Edition*. Wiley, 2011.